

Modification of ASTM B107 AZ31 alloy with TiO₂ particles using the dip-coating method

Modificación de la aleación ASTM B107 AZ31 con partículas de TiO₂ utilizando el método de recubrimiento por inmersión

DOI: <https://doi.org/10.17981/ingecuc.14.2.2018.04>

Artículo de investigación. Fecha de recepción: 28/02/2018. Fecha de aceptación: 16/06/2018

J. López H. 

Instituto Tecnológico Metropolitano ITM. Medellín (Colombia)
joeslopher@hotmail.com

V. Hernández-Montes 

Instituto Tecnológico Metropolitano ITM. Medellín (Colombia)
vanessahernandez@itm.edu.co

C. Betancur-Henao 

Instituto Tecnológico Metropolitano ITM. Medellín (Colombia)
claudiabetancur@itm.edu.co

J. F. Santa-Marín 

Instituto Tecnológico Metropolitano ITM. Medellín (Colombia)
Universidad Nacional de Colombia. Medellín (Colombia)
jfsanta@gmail.com

R. Buitrago-Sierra 

Instituto Tecnológico Metropolitano ITM. Medellín (Colombia)
robisonbuitrago@itm.edu.co

Para citar este artículo:

J. López H., V. Hernández-Montes, C. Betancur-Henao, J. F. Santa-Marín, R. Buitrago-Sierra "Modification of ASTM B107 AZ31 alloy with TiO₂ particles using the dip-coating method," *INGE CUC*, vol. 14, no. 2, pp. 45-54, 2018. DOI: <http://doi.org/10.17981/ingecuc.14.2.2018.04>

Abstract

Introduction– Magnesium alloys have been known for its biocompatible characteristics and tissue restoration properties. On the other hand, TiO₂ has been found to decrease the corrosion rates of the magnesium alloys.

Objective– In this work, the dip-coating technique was used to coat the magnesium alloy with TiO₂ particles in order to evaluate its corrosion resistance.

Methodology– The particles were analyzed by Scanning Electron Microscopy (SEM) and visual inspection. Additionally, hydrogen evolution tests were performed to understand the effect of adding TiO₂ in corrosion rates of Mg-alloys.

Results– The results showed the positive effect of TiO₂ in the improvement of the ASTM B107 AZ31B Mg alloys corrosion by an indirect measurement through hydrogen evolution tests. The bare ASTM B107 AZ31B showed a corrosion 29 times faster compared to the coated alloy. The thickness of the coatings obtained using the dip-coating method is thinner than 20 nm.

Conclusions– TiO₂ particles were aggregated on the surface of the ASTM B107 AZ31B alloy with a controlled speed. SEM images have shown the improvement of the coating when the H₂O concentration in the sol increased. Another important parameter is the withdrawal speed during the dip-coat process which was found to be better at a speed of 3mm/min. Hydrogen evolution in the acid solution showed that coated ASTM B107 AZ31B has less hydrogen production during the corrosion test. The dip-coating technique can also be used to coat polypropylene discs entirely.

Keywords– Dip-coating; corrosion, TiO₂ particles, Mg alloys, hydrogen evolution

Resumen

Introducción– Las aleaciones de magnesio son conocidas por sus características biocompatibles y propiedades de restauración de tejidos; por otro lado, se ha encontrado que el TiO₂ disminuye las velocidades de corrosión de las aleaciones de magnesio.

Objetivo– En este trabajo, la técnica de recubrimiento por inmersión se usó para recubrir una aleación de magnesio con partículas de TiO₂ y evaluar su comportamiento a corrosión.

Metodología– Las partículas se analizaron por microscopía electrónica de barrido (SEM) e inspección visual. Además, se realizaron pruebas de evolución de hidrógeno para comprender el efecto de la adición de TiO₂ en la velocidad de corrosión de la aleación de Mg.

Resultados– Los resultados mostraron el efecto positivo de TiO₂ en la mejora de la corrosión de aleaciones de ASTM B107 AZ31B Mg mediante una medición indirecta a través de pruebas de evolución de hidrógeno. La aleación ASTM B107 AZ31B sin recubrimiento muestra una corrosión 29 veces más rápida en comparación con la aleación recubierta. El espesor obtenido mediante el método de recubrimiento por inmersión es inferior a 20 nm.

Conclusiones– Las partículas de TiO₂ se agregaron en la superficie de la aleación ASTM B107 AZ31B con una velocidad controlada. Las imágenes SEM mostraron la mejora del recubrimiento cuando aumenta la concentración de H₂O en el sol. Otro parámetro importante es la velocidad de extracción durante el proceso de recubrimiento por inmersión, que resultó ser mejor a una velocidad de 3 mm/min. La evolución del hidrógeno en la solución mostró que la aleación ASTM B107 AZ31B recubierta reportó menos producción de hidrógeno durante la prueba de corrosión. La técnica de recubrimiento por inmersión puede realizarse en polipropileno y, finalmente, obtener una superficie completamente recubierta.

Palabras clave– Recubrimientos por inmersión, corrosión, partículas de TiO₂, aleaciones de Mg, evolución del hidrógeno

I. INTRODUCTION

Several research studies have analyzed the biocompatibility of magnesium alloys. Some of these have compared them to traditional biomaterials such as titanium, Co-Cr-Ni and stainless-steel alloys [1], [2].

Magnesium alloys have attracted much attention of biomedical researchers due to its mechanical properties, which are similar to those of the bone [3]. Some papers have shown the importance of magnesium for bone and tissue restoration because of osteoblast activation using a chondrocyte column fixation necessary for new bone tissue formation [4]. In addition, as an absorbable material, it could be used to avoid a secondary surgery to remove the implant when a bone fixation surgery is performed [5]. Moreover, traumatic effects and other related problems such as bone deformation and low function recovery rate are avoided [6], [7]. Even though, magnesium alloys are biocompatible, they present a low corrosion resistance hindering the application of these promising materials. Accordingly, it is necessary to find alternative methods and techniques to reduce the corrosion rate for biomedical application [7]-[9] Co-Cr-Ni alloy and titanium implants. Till date, extensive mechanical, in-vitro and in-vivo studies have been done to improve the biomedical performance of Mg alloys through alloying, processing conditions, surface modification etc. This review comprehensively describes the strategies for improving the mechanical and degradation performance of Mg alloys through properly tailoring the composition of alloying elements, reinforcements and processing techniques. It also highlights the status and progress of research in to (i).

Coatings with nanoparticles have been one of the most used and attractive methods to improve corrosion resistance of biomaterials [10], [11] an anticorrosive and antimicrobial coating was prepared on Mg alloy surface by layer-by-layer (LbL). Particles not only provide corrosion protection, but they also provide biocompatibility, and they are suitable for different ceramic and polymer coatings for biomedical application [12]-[14] which enables their use in medical applications and accounts for their extensive use as implant materials in the last 50 years. Currently, a large amount of research is being carried out in order to determine the optimal surface topography for use in bioapplications, and thus the emphasis is on nanotechnology for biomedical applications. It was recently shown that titanium implants with rough surface topography and free energy increase osteoblast adhesion, maturation and subsequent bone formation. Furthermore, the adhesion

of different cell lines to the surface of titanium implants is influenced by the surface characteristics of titanium; namely topography, charge distribution and chemistry. The present review article focuses on the specific nanotopography of titanium, i.e. titanium dioxide (TiO₂). Polypropylene has also been used in a wide range of applications such as medical devices, filters, food packaging material, and water purification membranes. In those applications surface properties are improved by coatings [15]-[18].

In order to coat a substrate surface, there are in the literature several techniques to facilitate particle fixation such as, chemical vapor deposition, dip-coating, spray coating, sputtering, laser deposition, among others [19], [20].

A method with outstanding results is the dip-coating technique. In this technique, a coating is formed by the immersion and subsequent withdrawal of a material into a sol containing the particles. Even though dip-coating is a low-cost method, the quality of the obtained coat is the result of various processes as particle aggregation, adherence and adsorption on the surface and it is controlled by some variables, such as: withdrawal speed, particle concentration in the sol, surface area, surface tension, capillarity, solvent removal temperature, among others [21], [22]. From literature, one of the most determinant variables is the withdrawal speed and it has been shown that, the lower the velocity (for a controlled solution viscosity), the better the results obtained for the coat thickness and particle aggregation [23]-[25].

In this work, ASTM B107 AZ31B magnesium alloy substrates and polypropylene discs were modified with TiO₂ particles by the dip-coating method. Different withdrawal speeds and water-ethanol ratio for the sol in the dip-coating process were evaluated. Also, the protection against corrosion of magnesium was studied using the hydrogen evolution method.

II. METHODOLOGY

A. Sample preparation

ASTM B107 AZ31B (from now on AZ31) magnesium discs were obtained from a 1" diameter bar. The discs (14 mm diameter and 4 mm of thickness) were obtained by using a lathe. Polypropylene discs were obtained from a 4 mm polypropylene sheet by drilling a hole with a 5/8" saw.

All discs were polished using 320, 400, 600 and 1000 sand paper before applying the coatings. The discs were lubricated with ethanol during the process and cleaned with a mixture of ethanol and glycerin in an ultrasonic bath (Branson 1800 brand) for 30 minutes. Subsequently, all discs

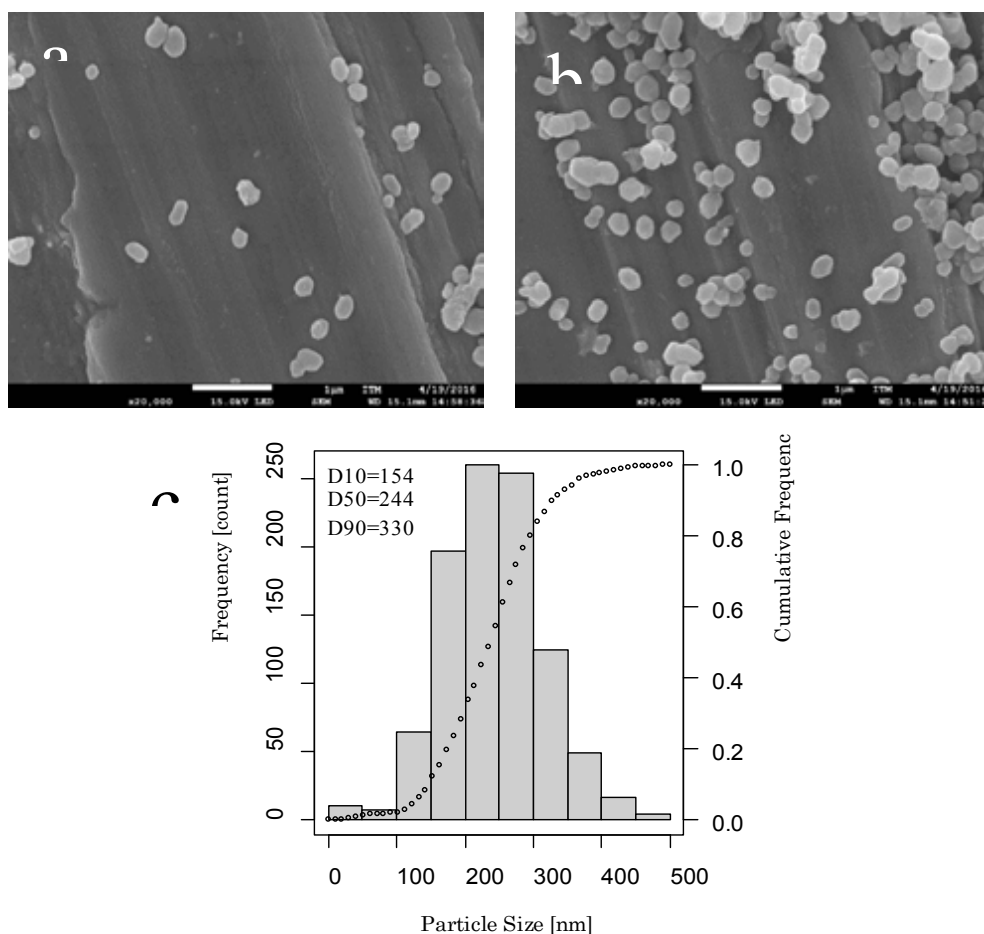
were exposed to a 2.5 M NaOH solution at a 70 °C for 15 minutes in order to remove the glycerin residuals from the surface. After that, the discs were washed with abundant deionized water and dried in a Binder incubator. In addition, the discs were treated with a 0.1 M solution of HNO₃ at room temperature for 15 seconds to remove the ions and free radicals exposed on the surface. The NaOH and HNO₃ procedures were performed inside an extractor cabin [26].

Commercial particles of TiO₂ were used (TIO-NA 595, functionalized with Alumina, Zirconia and O-H groups, according to the datasheet) to coat the substrates. A starting solution for the dip-coating process was prepared by mixing 3 g of TiO₂ particles and different ratios of water/ethanol solutions (70/30, 30/70 and 100/0 % vol) with magnetic stirring for 2 hours. The dip-coating procedure was performed in a Shimadzu AGX100 Universal machine in order to control the dip-coating process. The coatings were prepared using several speeds of withdrawal (1, 3, 10, 125, 300 and 600 mm/min) during the coating process.

B. Sample characterization

Phase identification and lattice structure of the TIO-NA 595 were characterized using an X-ray diffractometer (PANalytical X'Pert PRO MPD) operated with Cu K α radiation ($\lambda = 1,54 \text{ \AA}$) that the X-ray source generated at 45 keV and 40 mA. The size and shape of the particles were observed using a scanning electron microscope JEOL 7100F (FE-SEM). All the coatings were characterized using stereo microscope (Leica EZ4D), FE-SEM and the chemical composition was obtained by an energy dispersive analysis (EDS).

Corrosion tests were performed by measuring the volume of hydrogen produced as an indirect measurement of the discs' corrosion according to [27]-[29]. Therefore, samples were immersed in a 0.005 M HCl solution at pH 2.3 during 8 hours and, during the tests, the amount of water displaced by the hydrogen produced during the corrosion test was measured. The coatings used in this test were obtained using the best conditions of withdrawal and the water/alcohol ratio previously obtained.



Figs. 1 (a)-(b). SEM images of TiO₂ particles and (c) histogram of particle size distribution. Source: Authors.

III. RESULTS

Fig. 1 (a-b) show a SEM image obtained from the titanium dioxide particles. The image reveals that the particles have a spherical morphology. Fig. 1c shows a histogram representing the particle-size distribution. The particle size analysis was completed by analyzing dispersed particles with the SEM and using the ImageJ software. A total of 990 particles were measured. The D90, D50 and D10 values are also shown in the same figure (fig. 1C). The histogram shows that D50 is 244 nm and, since the value represents 50 % of particles, it is considered as the median diameter. Similarly, D10 and D90 indicate that 10 % of particles are below 154 nm and 90 % of particles are below 330 nm, respectively. These results indicate that the sizes of the particles are in the micron range. Fig. 2 shows the X-ray diffraction pattern of the particles. The analysis of TiO₂ nanoparticles showed rutile-phase TiO₂, with characteristic diffraction peaks of 2θ values at 25°, 41°, 49° and 54° attributed to the (101), (111), (200) and (211) planes, respectively. These results are consistent with the literature [30].

Fig. 3 (a)-(c) show the SEM images of AZ31 surface coated with TiO₂ particles when the ratio of water and ethanol is modified. A first test using a with-

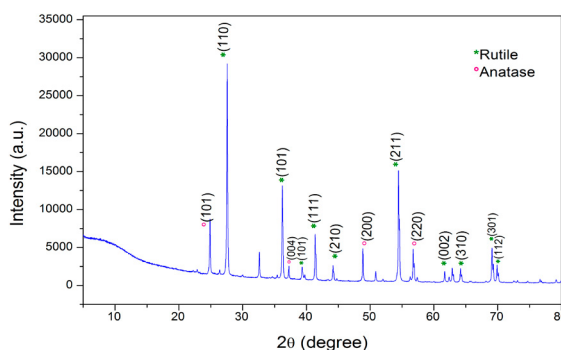


Fig. 2. XRD spectra of TiO₂ commercial particles. Source: Authors.

drawal speed of 3 mm/min and a sol with 70/30 % ethanol/water (fig. 3a) shows a poor adherence of the particles to the substrate surface with large zones showing no formation of the coating. It is visible that these spots have parallel lines corresponding to the sanded surface and the particle distribution is completely random. Some areas have no particles on it and some others have a cluster of TiO₂ particles at the surface. The higher the ethanol concentration in the solvent, the lesser the particles interact with the surface. Accordingly, the H₂O percentage in the solvent was increased.

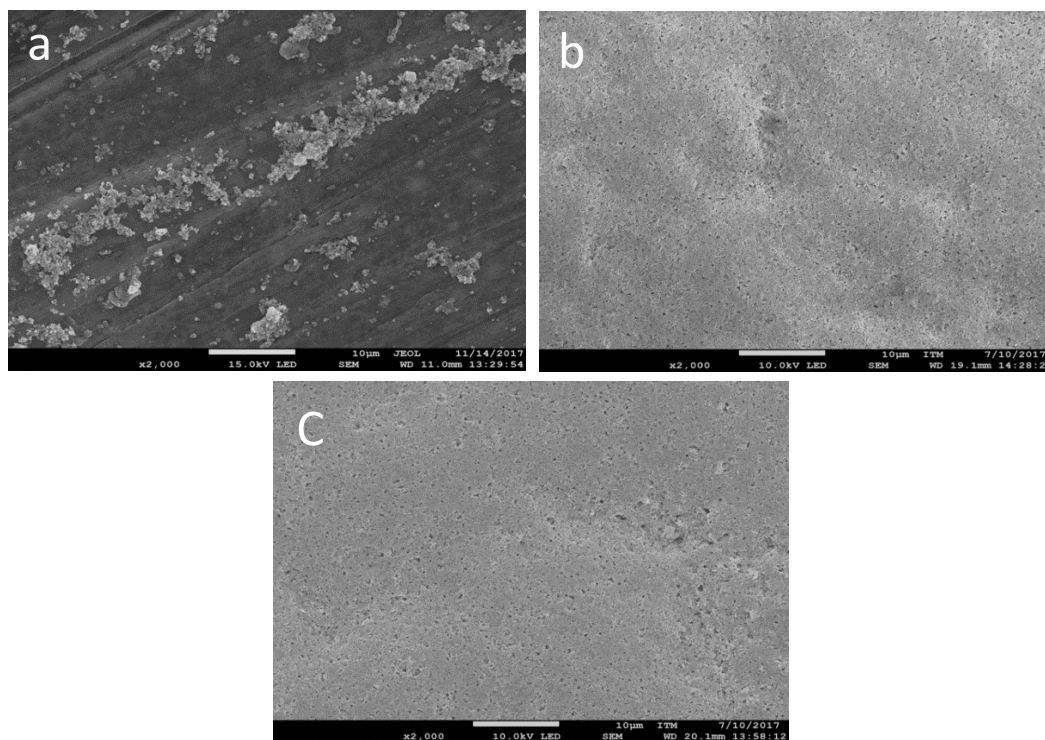


Fig. 3. AZ31 dip-coating with 595 TiO₂ sol solvent concentration test ethanol/water SEM, a) 70%/30% ethanol/water, b) 30%/70% ethanol/water, c) 100% water. Source: Authors.

The SEM images from the surfaces with high water content showed TiO_2 particles aggregated on the surface and the AZ31 surface was not exposed (Figs. 1 [b-c]). This result could be related to the hydration layer formed around the commercial TiO_2 . Alumina covering on commercial TiO_2 generates a hydration layer. That layer generates aggregates and affects the flow behavior of the suspensions. Moreover, the hydrated clusters alter the effective solid content and the viscosity of the suspensions [31]. When the viscosity increases, the number of particles in the meniscus is also increased, and during substrate withdrawal these particles are more easily aggregated at the surfaces improving the covering.

Sample images obtained by the stereomicroscope (Figs. 4 [a-c]) confirmed the results from the SEM images. The characteristic light reflection of the AZ31 with a poor covering is observed in the first case (Fig. 4a). On the other hand, a white coat, characteristic of the TiO_2 particles, and a rough surface is observed, hence, proving the other two samples (Figs. 4 [b-c]) to be a heterogeneous surface. This result can be explained by the high capillarity of water against the ethanol. From samples obtained with a high-water concentration, a better interaction of TiO_2 nanoparticles and the surface in this solvent was observed through Van der Waals forces. Accordingly, water was selected as the appropriate solvent for the dip-coating process.

SEM images in Figs. 5(a)-(f) show the AZ31 coated surface obtained by the dip-coating method with several withdrawal speeds of 1, 3, 10, 125, 300 and 600 mm/min. In all cases, the coating formed on the surface was dried at 80 °C for 2 hours. From the results, 1 and 3 mm/min withdrawal speeds (Figs. 5 [a-b]) showed the most homogenous coat with less uncoated spots on the surface. On the other hand, results obtained when using the 10, 125, and 600 mm/min procedure (Figs. 5 [c-f]) showed large zones without particles and a non-complete coating is observed; in addition, some agglomerates could be observed. Similar results have been previously reported in the literature [32].

According to the literature, at a lower withdrawal speed, the evaporation of the solution is faster, increasing the particles in the upper part of the meniscus formed when the substrate is moving upwards, thus, favoring layer formation [33], [34]. The use of alcohol and water mixtures also alters the evaporation rate and the surface tension for the particles suspended in the sol, varying the film shape by modifications in the capillarity [34]. Therefore, the best coatings were obtained using a withdrawal speed of 3 mm / min and in a water solution.

Low withdrawal speed favors the interaction between the alloy surface and the suspended particles in the fluid, but as the speed increases, one of the obstacles is the entrapment of air bubbles, decreasing the quality of the coatings. When the coating dries, these bubbles become pits with craters.

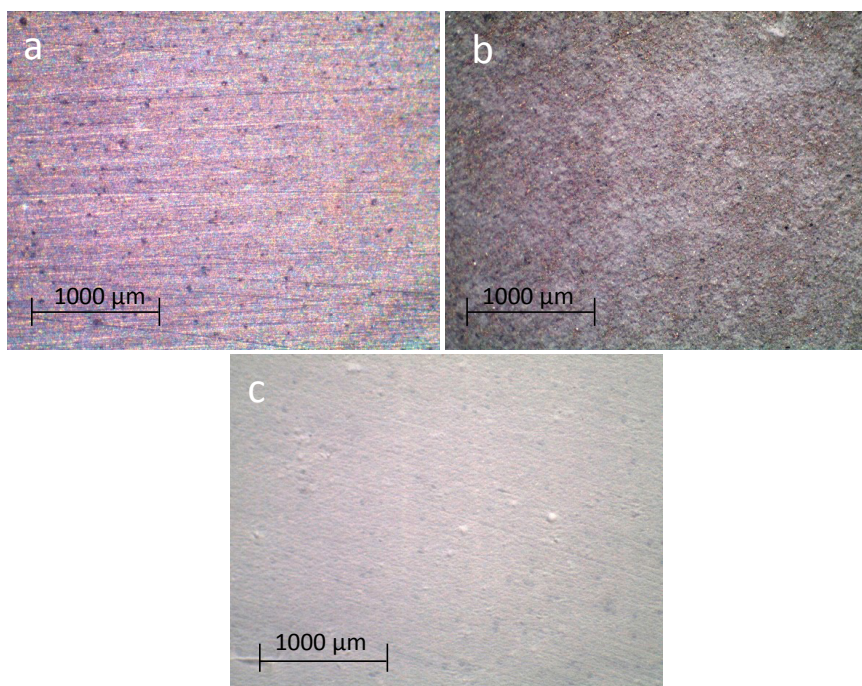


Fig. 4. Stereoscopic images of AZ31 dip-coating with 595 TiO_2 sol solvent concentration test ethanol/water, a) Bare surface, b) 70%/30% water/ethanol sol dip-coating, c) 100% water sol dip-coating.

Source: Authors.

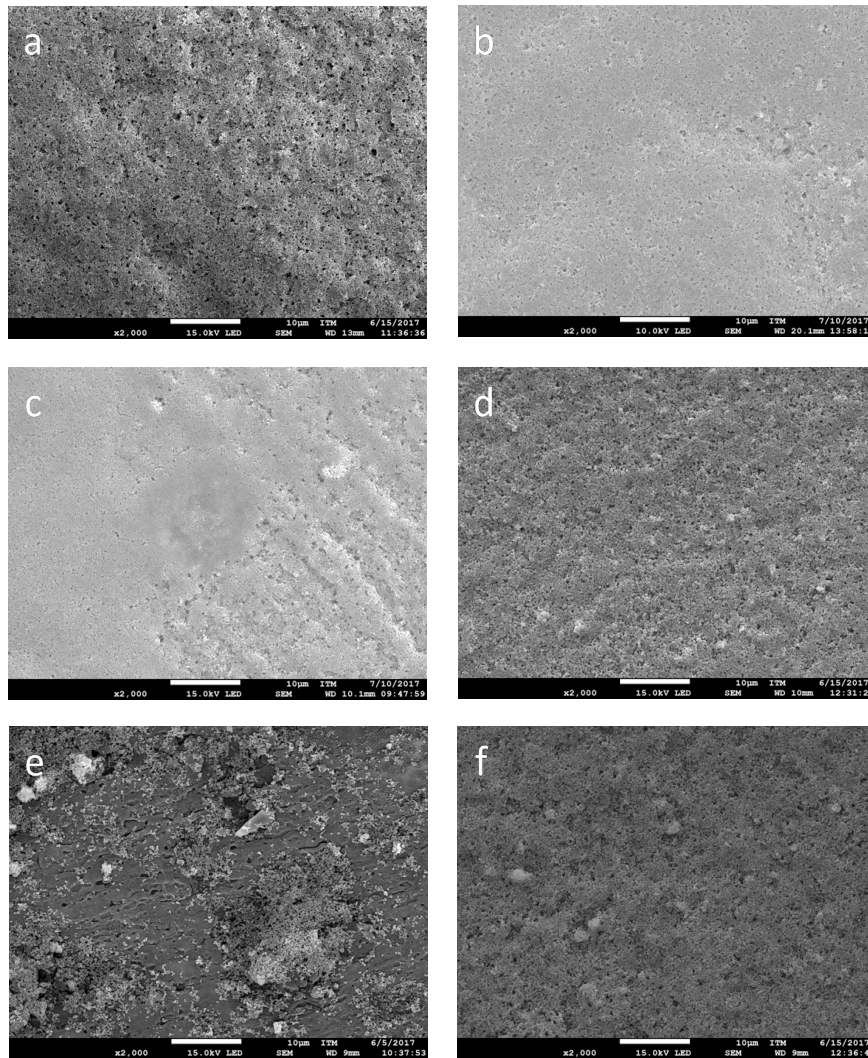


Fig. 5. SEM images of AZ31 dip-coating in H₂O 595 TiO₂ sol withdrawal speed test with a x2,000 magnification rate, a) 1 mm/min, b) 3 mm/min, c) 10 mm/min, d) 125 mm/min, e) 300 mm/min, f) 600 mm/min. Source: Authors.

Fig. 6 shows a SEM image of a transverse section of coatings with TiO₂ on AZ31 (a). The chemical composition of the coating was analyzed by EDS. The same figure shows the elemental mapping images of O, Ti, Al, and Mg (shown in Fig. 6 [b, c, d, e]). EDS analysis confirmed the presence of the characteristic elements of titanium dioxide (oxygen and titanium) on AZ31 surface. The images show the presence of Al both in the substrate material and in the coating with titanium dioxide. This is attributed to the elemental composition of the AZ31 alloy that has approximately 3% wt. of Al, and additionally to the presence of this element on the surface of the TiO₂ particles, as described by the manufacturer. The elements present in the AZ31 alloy have a very low weight percentage which makes it difficult to detect them by EDS, given the detection limits of the technique.

Furthermore, thickness of the coating is one of the most important parameters during the dip-coating process. Some authors have reported for hydroxyapatite coats that the thinner the coating, the better its mechanical properties. Since in some cases the coating is dissolved inside the body, by increasing the thickness ($\geq 50 \mu\text{m}$) the resorption problem can be solved by providing mechanical strength to the system [35], [36]. Fig. 6 shows the transverse section of a coating to analyze the thickness of the formed coat. The minimum thickness found was 6.1 μm and the maximum 19.6 μm with a standard deviation of 4.4 μm and a mean of 9.9 μm . Even though the thickness is not uniform, the coating is enough to withstand aggressive environments (pH < 2.3), as evidenced by the hydrogen evolution test shown below.

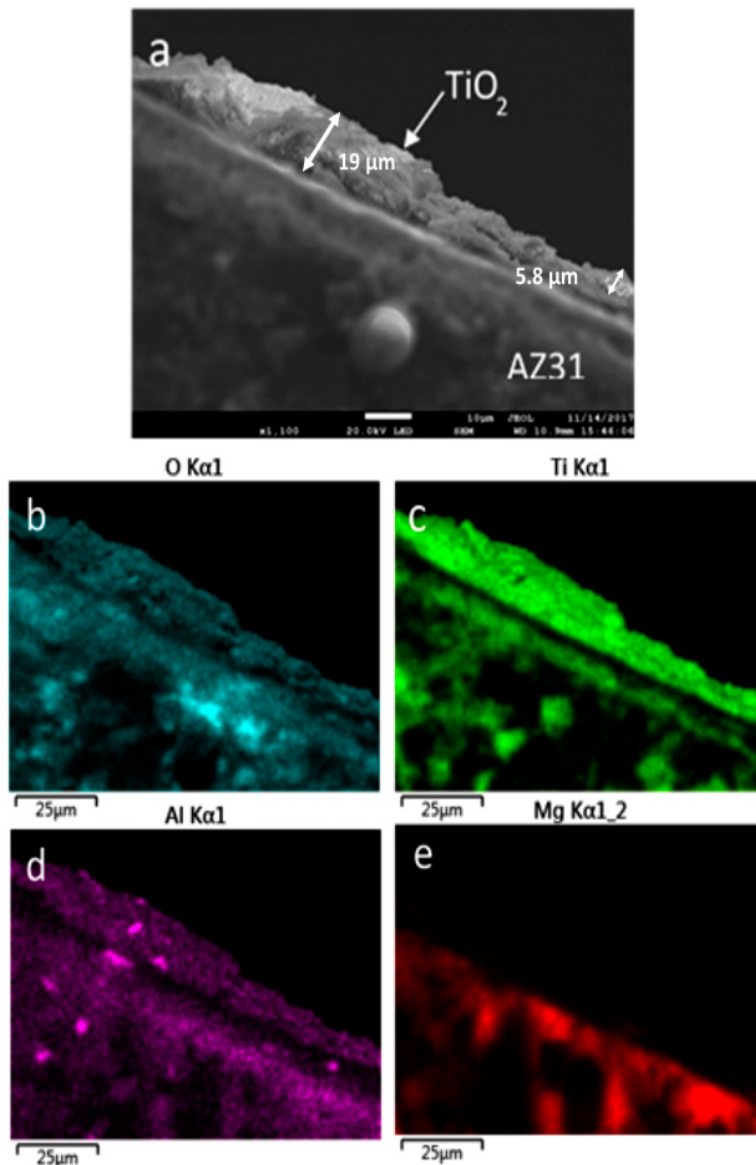


Fig. 6. AZ31 SEM image, film thickness and AZ31 EDS film thickness, a) Oxygen, b) Titanium, c) Aluminum, d) Magnesium. Source: Authors.

Corrosion tests were completed by performing hydrogen evolution tests. Fig. 7 shows the hydrogen evolution of the uncoated AZ31 sample and an AZ31 coated with TiO_2 . As seen for the bare AZ31, the collected data show an increasing hydrogen volume with an exponential behavior. After 480 min (8h), the amount of fluid displaced is higher than 140 mL, while the AZ31 coated with the TiO_2 particles shows a stable behavior with a 0 mL of fluid displacement after 90 min. Afterwards, a minimum

displacement is obtained after 400 min. Later on, the displaced volume increased slightly, although it never reached 20 mL. Since the amount of hydrogen collected is equal to the amount of dissolved magnesium, this result showed that the hydrogen evolution of the magnesium coated with titanium dioxide is the lowest. When that result is compared to the hydrogen evolution of the bare alloys, the best corrosion resistance is expected from coated magnesium.

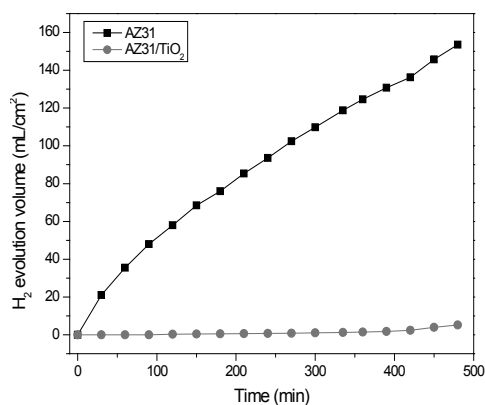


Fig. 7. Hydrogen evolution test for unmodified AZ31; AZ31 coated with TiO₂. Source: Authors.

From the previous results, the same conditions were selected to study the dip-coating method by using polypropylene discs as the substrate. Figs. 8(a)-(c) show the SEM images at different magnification rates (x2,000 and x10,000) of the polypropylene discs surface fully coated with the TiO₂ particles using a water solution of TiO₂ particles and a withdrawal speed of 3 mm/min. The figures 8b and 8c provide a closer view of the coating, showing the particles under the top of the layer. The polypropylene surface is no longer visible and is coated with the TiO₂ 595 particles. These results confirm the effectivity and versatility of the dip-coating method to cover surfaces for polymers.

IV. CONCLUSIONS

TiO₂ coatings were applied onto ASTM B107 AZ31 and polypropylene (PP) substrates through the dip-coating method. TiO₂ particles were aggregated on the surface of the ASTM B107 AZ31 alloy with a controlled speed, and the hydrogen evolution was evaluated using a HCl solution.

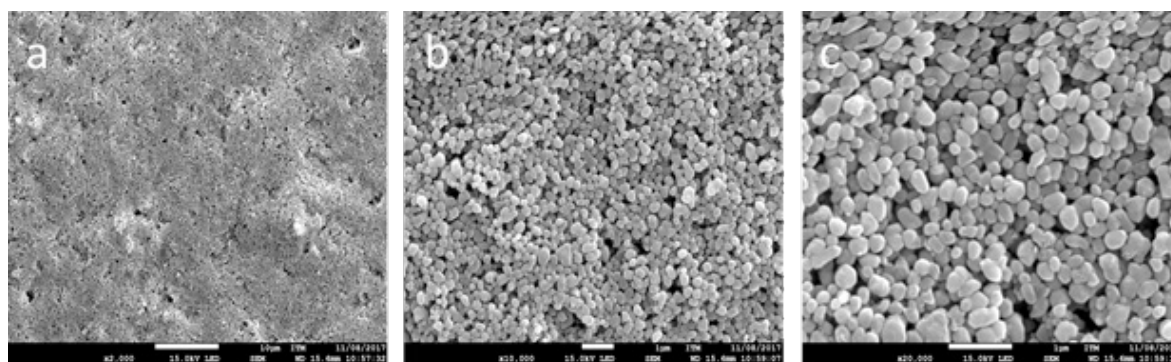


Fig. 8. SEM images of polypropylene dip-coating in H₂O 595 TiO₂ sol 3 mm/min withdrawal speed, a) x2,000 magnification rate, b) x10,000 magnification rate, c) x20,000 magnification rate. Source: Authors.

SEM images have shown the improvement of the coating when the H₂O concentration in the sol increased. Another important parameter is the withdrawal speed during the dip-coating process, which was found to be better at a speed of 3 mm/min. Hydrogen evolution in the acid solution showed that coated ASTM B107 AZ31B has 20 times less hydrogen production during the corrosion test.

Additional tests are required to conclude about the corrosion resistance in a physiological environment (pH 7.3–7.5) using a simulated body fluid immersion to obtain the results.

Polypropylene discs were also coated with TiO₂ by the dip-coating technique, demonstrating that the coating parameters found for coatings with TiO₂ 595 particles on magnesium can be successfully used in other types of materials.

V. ACKNOWLEDGEMENTS

The authors would like to acknowledge the Instituto Tecnológico Metropolitano (ITM) for the project: “Modificación superficial del magnesio AZ31 para aplicaciones en biomateriales” (january, 2018–december, 2019) and the Convocatoria Jóvenes Investigadores Colciencias 2017 (february, 2017–november, 2017). The authors would also like to thank the polymers laboratory, the microscopy laboratory and the Advanced Material and Energy Research Group (MATyER) from Instituto Tecnológico Metropolitano for their support.

REFERENCES

- [1] S. Agarwal, J. Curtin, B. Duffy, and S. Jaiswal, “Biodegradable magnesium alloys for orthopaedic applications: A review on corrosion, biocompatibility and surface modifications,” *Mater. Sci. Eng. C*, vol. 68, pp. 948–963, Nov. 2016. <https://doi.org/10.1016/j.msec.2016.06.020>
- [2] J. Fei et al., “Biocompatibility and neurotoxicity of magnesium alloys potentially used for neural repairs,” *Mater. Sci. Eng. C*, vol. 78, pp. 1155–1163, Sep. 2017. <https://doi.org/10.1016/j.msec.2017.04.106>

- [3] Y. Liu, Y. Liu, N. Liao, F. Cui, M. Park, and H.-Y. Kim, "Fabrication and durable antibacterial properties of electrospun chitosan nanofibers with silver nanoparticles," *Int. J. Biol. Macromol.*, vol. 79, pp. 638–643, 2015. <https://doi.org/10.1016/j.jbiomac.2015.05.058>
- [4] M. Razavi et al., "In vivo study of nanostructured diopside (CaMgSi₂O₆) coating on magnesium alloy as biodegradable orthopedic implants," *Appl. Surf. Sci.*, vol. 313, pp. 60–66, Sep. 2014. <https://doi.org/10.1016/j.apsusc.2014.05.130>
- [5] R. Bertolini, S. Bruschi, A. Ghiotti, L. Pezzato, and M. Dabalà, "The Effect of Cooling Strategies and Machining Feed Rate on the Corrosion Behavior and Wettability of AZ31 Alloy for Biomedical Applications," *Procedia CIRP*, vol. 65, pp. 7–12, Jan. 2017. <https://doi.org/10.1016/j.procir.2017.03.168>
- [6] S. Castiglioni, A. Cazzaniga, W. Albisetti, and J. A. M. Maier, "Magnesium and osteoporosis: current state of knowledge and future research directions," *Nutrients*, vol. 5, no. 8, pp. 3022–33, Jul. 2013. <https://doi.org/10.3390/nu5083022>
- [7] R. Radha and D. Sreekanth, "Insight of magnesium alloys and composites for orthopedic implant applications – a review," *J. Magnes. Alloy.*, vol. 5, no. 3, pp. 286–312, 2017. <https://doi.org/10.1016/j.jma.2017.08.003>
- [8] M. Esmaily et al., "Fundamentals and advances in magnesium alloy corrosion," *Prog. Mater. Sci.*, vol. 89, pp. 92–193, Aug. 2017. <https://doi.org/10.1016/j.pmatsci.2017.04.011>
- [9] I. A. Shahar, T. Hosaka, S. Yoshihara, and B. J. Macdonald, "Mechanical and Corrosion Properties of AZ31 Mg Alloy Processed by Equal-Channel Angular Pressing and Aging," *Procedia Eng.*, vol. 184, pp. 423–431, 2017. <https://doi.org/10.1016/j.proeng.2017.04.113>
- [10] X. Zhang et al., "Layer-by-layer assembly of silver nanoparticles embedded polyelectrolyte multilayer on magnesium alloy with enhanced antibacterial property," *Surf. Coatings Technol.*, vol. 286, pp. 103–112, Jan. 2016. <https://doi.org/10.1016/j.surfcoat.2015.12.018>
- [11] R.-G. Hu, S. Zhang, J.-F. Bu, C.-J. Lin, and G.-L. Song, "Recent progress in corrosion protection of magnesium alloys by organic coatings," *Prog. Org. Coatings*, vol. 73, no. 2–3, pp. 129–141, Feb. 2012. <https://doi.org/10.1016/j.porgcoat.2011.10.011>
- [12] M. Kulkarni et al., "Titanium nanostructures for biomedical applications," *Nanotechnology*, vol. 26, no. 6, p. 062002, Feb. 2015. <https://doi.org/10.1088/0957-4484/26/6/062002>
- [13] A. M. Khorasani, M. Goldberg, E. H. Doeven, and G. Littlefair, "Titanium in Biomedical Applications -Properties and Fabrication: a Review," *Tissue Eng. J. Biomater. Tissue Eng.*, vol. 5, no. 5, pp. 593–619, 2015. <https://doi.org/10.1166/jbt.2015.1361>
- [14] M. A. Shaheed and F. H. Hussein, "Preparation and Applications of Titanium Dioxide and Zinc Oxide Nanoparticles," *J. Environ. Anal. Chem.*, vol. 02, no. 01, 2014. <https://doi.org/10.4172/2380-2391.1000e109>
- [15] A. Saffar, P. J. Carreau, M. R. Kamal, and A. Aji, "Hydrophilic modification of polypropylene microporous membranes by grafting TiO₂ nanoparticles with acrylic acid groups on the surface," *Polymer (Guildf.)*, vol. 55, no. 23, pp. 6069–6075, Nov. 2014. <https://doi.org/10.1016/j.polymer.2014.09.069>
- [16] M. Lu et al., "Photo- and thermo-oxidative aging of polypropylene filled with surface modified fumed nanosilica," *Compos. Commun.*, vol. 3, pp. 51–58, Mar. 2017. <https://doi.org/10.1016/j.coco.2017.02.004>
- [17] S. C. Tjong, K. Yeung, H. M. Wong, and C. Z. Liao, "The development, fabrication, and material characterization of polypropylene composites reinforced with carbon nanofiber and hydroxyapatite nanorod hybrid fillers," *Int. J. Nanomedicine*, vol. 9, p. 1299, Mar. 2014. <https://doi.org/10.2147/IJN.S58332>
- [18] Y. Liu and M. Wang, "Fabrication and characteristics of hydroxyapatite reinforced polypropylene as a bone analogue biomaterial," *J. Appl. Polym. Sci.*, vol. 106, no. 4, pp. 2780–2790, Nov. 2007. <https://doi.org/10.1002/app.26917>
- [19] K. Seshan, Handbook of thin film deposition: techniques, processes, and technologies. William Andrew, 2012.
- [20] P. Saravanan, M. Ganapathy, A. Charles, S. Tamilselvan, and R. Jeyasekaran, "Electrical properties of green synthesized TiO₂ nanoparticles," *Adv. Appl. Sci. Res.*, vol. 7, no. 3, pp. 158–168, 2016.
- [21] M. Poté, (2016). Dip Coating vs. Spin Coating. Satisloh Italy S.r.l. [Online]. Available http://www.satisloh.com/fileadmin/contents/Whitepaper/Dip-Coating-vs-Spin-Coating_EN.pdf
- [22] S. Thirugnanaselvi, S. Kuttirani, and A. R. Emelda, "Effect of Schiff base as corrosion inhibitor on AZ31 magnesium alloy in hydrochloric acid solution," *Trans. Nonferrous Met. Soc. China*, vol. 24, no. 6, pp. 1969–1977, Jul. 2014. [https://doi.org/10.1016/S1003-6326\(14\)63278-7](https://doi.org/10.1016/S1003-6326(14)63278-7)
- [23] T. Schneller, R. Waser, M. Kosec, and D. Payne Editors, Chemical Solution Deposition of Functional Oxide Thin Films. New York: Springer, 2013.
- [24] V. G. Parale, D. B. Mahadik, V. D. Phadtare, A. A. Pisal, H. H. Park, and S. B. Wategaonkar, "Dip Coated Superhydrophobic and Anticorrosive Silica Coatings," *Int. J. Mater. Sci. Eng.*, vol. 4, no. 1, pp. 60–68, 2016.
- [25] X. Wang, F. Shi, X. Gao, C. Fan, W. Huang, and X. Feng, "A sol-gel dip/spin coating method to prepare titanium oxide films," *Thin Solid Films*, vol. 548, pp. 34–39, 2013. <https://doi.org/10.1016/j.tsf.2013.08.056>
- [26] Y. Reyes, A. Durán, and Y. Castro, "Glass-like cerium sol-gel coatings on AZ31B magnesium alloy for controlling the biodegradation of temporary implants," *Surf. Coatings Technol.*, vol. 307, no. Part A, pp. 574–582, 2016.
- [27] N. Van Phuong, M. Gupta, and S. Moon, "Enhanced corrosion performance of magnesium phosphate conversion coating on AZ31 magnesium alloy," *Trans. Nonferrous Met. Soc. China*, vol. 27, no. 5, pp. 1087–1095, May 2017. [https://doi.org/10.1016/S1003-6326\(17\)60127-4](https://doi.org/10.1016/S1003-6326(17)60127-4)
- [28] G. S. Frankel, A. Samaniego, and N. Birbilis, "Evolution of hydrogen at dissolving magnesium surfaces," *Corros. Sci.*, vol. 70, pp. 104–111, May 2013. <https://doi.org/10.1016/j.corsci.2013.01.017>
- [29] N. T. Kirkland, N. Birbilis, and M. P. Staiger, "Assessing the corrosion of biodegradable magnesium implants: A critical review of current methodologies and their limitations," *Acta Biomater.*, vol. 8, no. 3, pp. 925–936, Mar. 2012. <https://doi.org/10.1016/j.actbio.2011.11.014>
- [30] H.-S. Chen, C. Su, J.-L. Chen, T.-Y. Yang, N.-M. Hsu, and W.-R. Li, "Preparation and Characterization of Pure Rutile TiO₂ Nanoparticles for Photocatalytic Study and Thin Films for Dye-Sensitized Solar Cells," *J. Nanomater.*, vol. 2011, pp. 1–8, Nov. 2011. <https://doi.org/10.1155/2011/510237>
- [31] E. Firlar, S. Çınar, S. Kashyap, M. Akinc, and T. Prozorov, "Direct Visualization of the Hydration Layer on Alumina Nanoparticles with the Fluid Cell STEM in situ," *Sci. Rep.*, vol. 5, no. 1, p. 9830, Sep. 2015. <https://doi.org/10.1038/srep09830>
- [32] O. Coahu and H. Benkreira, "Air entrainment in angled dip coating," *Chem. Eng. Sci.*, vol. 53, no. 3, pp. 533–540, Feb. 1998. [https://doi.org/10.1016/S0009-2509\(97\)00323-0](https://doi.org/10.1016/S0009-2509(97)00323-0)
- [33] C. J. Brinker, G. C. Frye, A. J. Hurd, and C. S. Ashley, "Fundamentals of sol-gel dip coating," *Thin Solid Films*, vol. 201, no. 1, pp. 97–108, Jun. 1991. [https://doi.org/10.1016/0040-6090\(91\)90158-T](https://doi.org/10.1016/0040-6090(91)90158-T)
- [34] G. Berteloot, A. Daerr, F. Lequeux, and L. Limat, "Dip coating with colloids and evaporation," *Chem. Eng. Process. Process Intensif.*, vol. 68, pp. 69–73, Jun. 2013. <https://doi.org/10.1016/j.cep.2012.09.001>
- [35] S. Zhang, Hydroxyapatite coatings for biomedical applications. Boca Raton: CRC Press, Taylor & Francis Group, 2013. <https://doi.org/10.1201/b14803>
- [36] M. Driver, "Coatings for biomedical applications," *Woodhead Publishing Series in Biomaterials*, 2012. pp. 353–366. <https://doi.org/10.1533/9780857093677>

Johan Esteban López Herrera, undergraduate student of biomedical engineering at the Instituto Tecnológico Metropolitano ITM (Medellín, Colombia). His research is focused in biomaterials, automation, sensors, production planning and scheduling, prosthetics and bionics. <https://orcid.org/0000-0001-7951-9099>

Vanessa Hernández-Montes, is a BSc. in Biomedical Eng. (2014), currently completing a MSc. Eng. degree in Biomedical Engineering at Instituto Tecnológico Metropolitano, Medellín, Colombia. She is a researcher for the Advanced Materials and Energy Research Group (MATyER) at Instituto Tecnológico Metropolitano. Her interests include biomaterials with emphasis on coatings and physical-chemical and mechanical characterization of materials. <https://orcid.org/0000-0002-4692-3623>

Claudia Betancur-Henao, is a BSc. in Biomedical Eng. (2014), currently completing a MSc. Eng. degree in Materials and Process Engineering at Universidad Nacional de Colombia. She is a researcher for the Advanced Materials and Energy Research Group (MATyER) at Instituto Tecnológico Metropolitano. Her interests include biomaterials with emphasis on physical-chemical and mechanical characterization of materials. <https://orcid.org/0000-0003-1345-9091>

Juan F. Santa-Marín, is a BSc. in Mechanical Eng. (2005), MSc. Eng in Materials and Process Engineering (2008) and PhD. in Engineering with emphasis on science and technology of materials (2013) from Universidad Nacional de Colombia. Currently, professor Santa is a researcher for the Advanced Materials and Energy Research Group (MATyER) at Instituto Tecnológico Metropolitano. His interests include materials in general with emphasis on wearing, processing, and physical-chemical and mechanical characterization of materials. He is coauthor of more than 12 international publications in international journals such as Tribology International, Wear, and others. <https://orcid.org/0000-0001-5781-672X>

Robison Buitrago-Sierra, Chemist (2007) from Universidad de Antioquia and PhD. in science of materials from Universidad de Alicante (2012). Currently, professor Buitrago is a researcher for the Advanced Materials and Energy Research Group (MATyER) at Instituto Tecnológico Metropolitano. His interests include. development and characterization of catalysts and nanostructured materials for different applications. <https://orcid.org/0000-0002-5995-4031>